Nanotechnology **21** (2010) 125302 (5pp) doi:10.1088/0957-4484/21/12/125302

Nanoscale sharpening tips of vapor–liquid–solid grown silicon microwire arrays

Akihiro Goryu, Akihito Ikedo, Makoto Ishida and Takeshi Kawano

Electrical and Electronic Engineering, Toyohashi University of Technology, Toyohashi, Aichi, Japan

E-mail: kawano@eee.tut.ac.jp

Received 8 January 2010, in final form 9 February 2010
Published 2 March 2010
Online at stacks.iop.org/Nano/21/125302

Abstract

We developed out-of-plane, high aspect ratio, nanoscale tip silicon microwire arrays for application to penetrating, multisite, nanoscale biological sensors. Silicon microwire arrays selectively grown by gold-catalyzed vapor–liquid–solid growth of silicon can be formed to create sharpened nanotips with a tip diameter of less than 100 nm by utilizing batch-processed silicon chemical etching for only 1–3 min. The tip angles achieved ranged from 11° to 38°. The nanotip silicon microwires can perform gelatin penetration without wire breakdown, indicating their potential penetrating capability for measurements inside biological tissues.

(Some figures in this article are in colour only in the electronic version)

1. Introduction

Penetrating nanoscale one-dimensional devices, including silicon nanowires [1] and carbon nanotubes [2–4], have been fabricated for their potential applications to nanoscale biological experimental tools, such as intracellular analysis and intracellular delivery. For multisite electrical measurements of a neuron/cell complex with nanoscale resolution, a semiconducting nanowire-based planar field effect transistor array has been proposed. This array exhibits parallel nanoscale interfacing with neuron tissues and their networks [5–7]. These proposed nano-device structures will be required to combine both the penetration and the multisite effect, particularly in further measurements inside three-dimensional biological tissues, such as the brain cortex (overall thickness ∼2 mm) [8].

In recent advances in nanotechnology, high aspect ratio semiconducting nanowires/carbon nanotubes can be synthesized (e.g. millimeter-scale length silicon nanowires by vapor–liquid–solid (VLS) growth [9] and carbon nanotubes by the water-assisted synthesis [10]). Nanowires/nanotubes with a length of several hundred microns or longer degrade in their penetrating capability due to their bending and/or breakdown [11] during tissue penetration, making the targeted tissue cell impossible to reach. To create a penetrating multisite nanowire array inside tissue, we propose a high aspect ratio, microscale penetrating wire scaffold as a mechanical support, formed by the selective VLS growth of silicon microwires [12, 13]. In this approach, only the tip section is selectively sharpened to nanoscale dimensions (<100 nm in diameter at the tip) by controlling the chemical etching of silicon.

2. Fabrication of nanoscale tip silicon microprobe arrays

2.1. Fabrication

We start with a silicon (111) substrate consisting of silicon microwire arrays assembled by selective VLS growth, using Si_2H_6 as the silicon gas source at a pressure of 0.5 Pa at 700 °C [12, 13]. The diameters of the as-grown silicon wires were 2–4 μm, and all of the wires had a constant length of 30 μm, as shown in figure 1(a). Figures 1(b)–(e) show subsequent batch processes for forming nanotip silicon microwire arrays. First, the wires are spray-coated conformally with a photoresist (thickness = ∼3 μm) (AZ5218E, viscosity 40 cP) (figure 1(b)) [14]. Second, the tips of the wires are selectively exposed from the photoresist by plasma etching with $O_2 + CF_4$ (figure 1(c)). Third, the tips are wet etched with a $HF + HNO_3$ solution [15] at a constant temperature

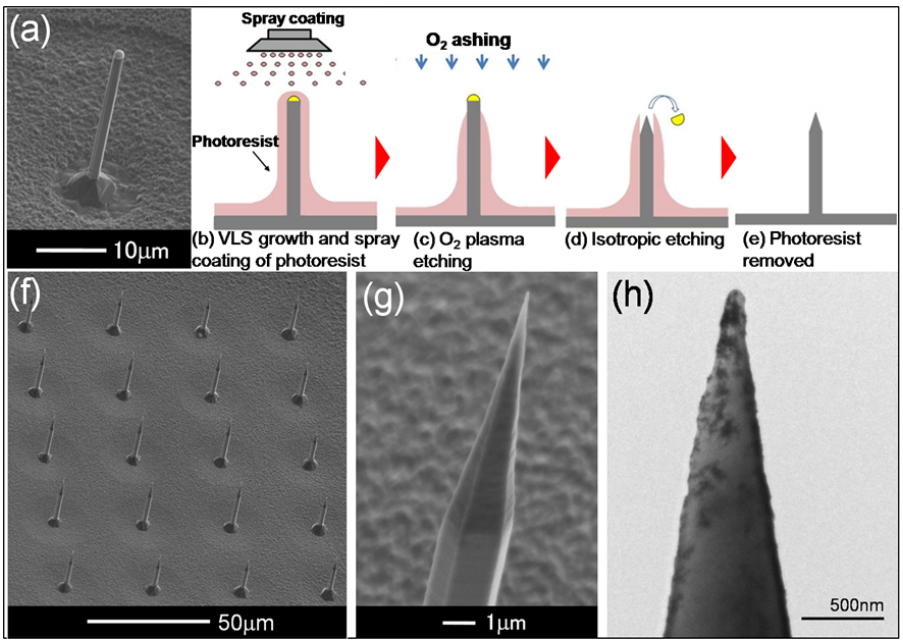

Figure 1. Fabrication of a nanotipped silicon microwire array. (a) The SEM image shows a single 30 μm long, 2 μm diameter silicon microwire in an array fabricated by vapor–liquid–solid growth. (b)–(e) The process flow of nanotip formation for the VLS grown silicon microwire by spray-coating of photoresist (b), tip exposure with oxygen plasma (c), silicon wet etching of a wire tip section (d) and photoresist removal (e). (f) SEM image of a nanotip silicon wire array formed from the same probes shown in image (a). (g) SEM image of the tip section of a wire in the array. (f) TEM image of the tip section shows a tip radius of curvature of 40 nm.

of 40 °C (etching time = 1–3 min) (figure 1(d)). Finally, the photoresist is removed with acetone (figure 1(e)). Figure 1(f) shows an SEM image of a nanotip silicon microwire array fabricated in this way, with a tip angle of 11°. For this array, an etching solution of HF(49%):HNO_3(61%):deionized water (DIW) (resistivity > 16 MΩ cm) = 1:50:25 was used for 2.5 min. Figure 1(g) gives a low-resolution TEM image of the tip section of a typical sharpened tip, indicating a tip radius of curvature of 40 nm. Note that all of the SEM images shown in this work were tilted at 45°, and the all of the length values, as well as the tip angles, of the wires in the SEM images were corrected for the tilt.

2.2. *Analysis of the tip formation*

For the quantitative analysis of the formation of the sharpened silicon tips, we performed timed experiments using different sharpening times of 1, 1.5, 2 and 3 min. These experiments were performed on four 4 μm-diameter silicon wires (wire length = 30 μm), using the same etching solution of HF:HNO_3:DIW = 1:50:25 at a constant temperature of 40 °C. Figures 2(a)–(d) are SEM images of the as-etched wire tip section with the photoresist and after photoresist removal for different sharpening times. We observed infiltration of the chemical solution at the interface between the wire walls and the photoresist, similar to etching a planar silicon substrate with patterned photoresist masking. Figure 2(e) shows illustrations of the time dependent tip shapes, where the accurate dimensions of the tip section are taken from SEM observations (figures 2(a)–(d)). Indeed, the results from SEM images and the illustrated tip shapes indicate the time dependent wire sharpening process, which is induced by both the lateral silicon etching and the vertical solution infiltration. Consequently, vertical solution infiltration defines the height of the cone-like shaped wire tip section, while the tip diameter is defined by lateral silicon etching. Figure 2(f) shows the relationship between the lateral silicon etching, a, and the vertical solution infiltration rate, b, as a function of sharpening process time (1–2 min), where all the data are taken from the same SEM observations (figures 2(a)–(d)). The silicon etching rate, a, exhibits linear behavior with a rate of 0.6 μm min^{-1}. In addition, the solution infiltration rate, b, also exhibits linear behavior with a rate of 5.1 μm min^{-1}, suggesting the whole process is controllable and repeatable, with constant etching and infiltration rates.

2.3. *Angle control*

Additionally, the proposed nanotip formation of silicon microwires has the advantage of variable tip angles. Angles of 11°–38° could be realized by utilizing different etching solutions. Three different concentration ratios of HF:HNO_3:DIW (1:50:0, 1:100:0 and 1:50:25) yielded silicon etching rates of 1.1, 0.7 and 0.6 μm min^{-1}, respectively, at 40 °C. To form a complete nanotip for a 1 μm radius silicon wire, we used an enhanced sharpening time of 1 min with a 1:50:0 solution. Similarly, sharpening times of 1.4 and 2.5 min were used for 1:100:0 and 1:50:25 solutions, respectively, on two other silicon wires with the same 1 μm radius. These differences in parameters resulted in

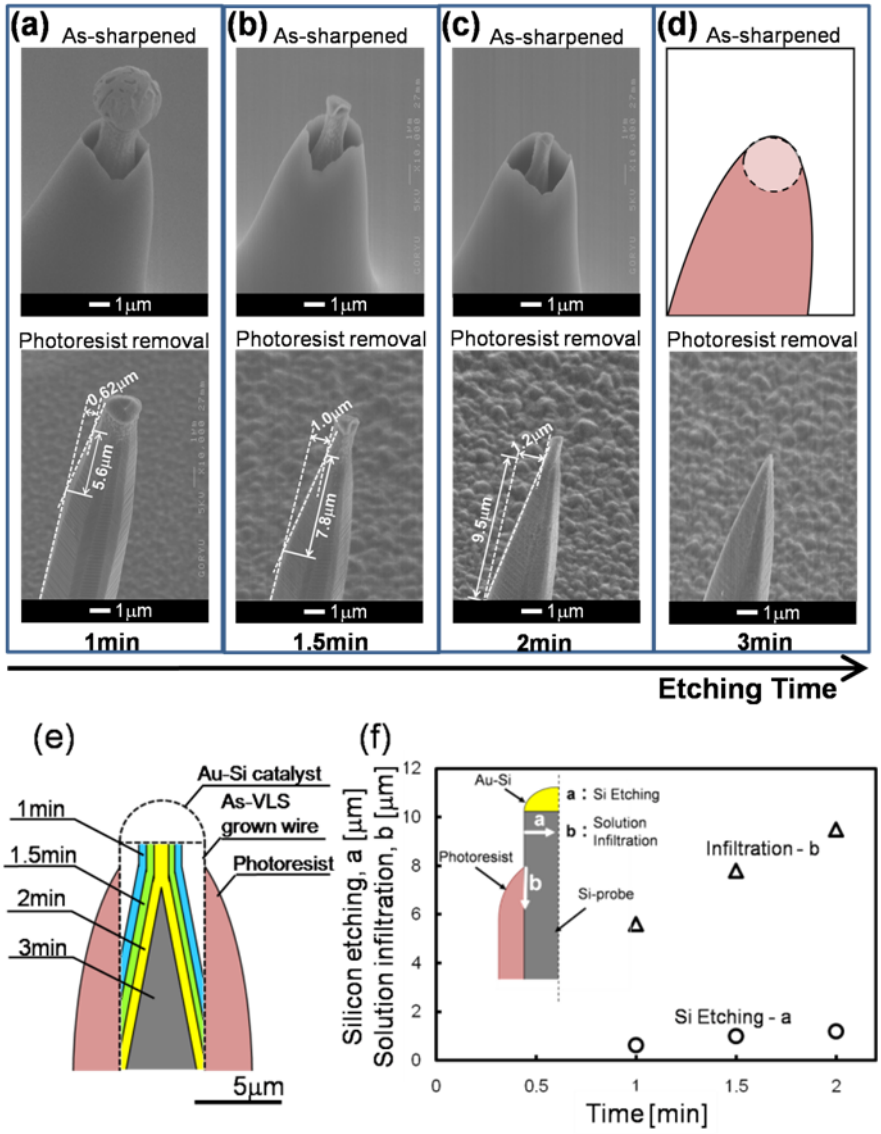

Figure 2. Sharpening-time-dependent tip shapes. SEM images and a schematic image of each as-sharpened tip section with photoresist are shown on the top, and each true tip SEM image after the photoresist removal is shown on the bottom. Sharpening times are (a) 1 min, (b) 1.5 min, (c) 2 min, and (d) 3 min. (e) Illustration of the time dependent nanoscale sharpening process. The dimensions of the tip sections are taken from the SEM images (a)–(d). (f) Measured silicon etching rate, a, and solution infiltration rate, b, as a function of sharpening process time. The data are also taken from the same SEM images (a)–(c). The inset shows a schematic of lateral silicon etching, a, and vertical solution infiltration, b.

tip angles of 38°, 27° and 11°, as shown in the SEM images in figures 3(a) and (b). To support the finding that the change in the tip angle is due only to the ratio of components of the etching solution (etching rate), the solution-independent infiltration rate was compared between $HF:HNO_3:DIW = 1:50:10$ and 1:50:25, and no significant solution dependence was observed. Table 1 summarizes the experimental results for different nanotip angles using the aforementioned sharpening parameters. Further reduced tip angles (<11°) would be possible by utilizing a slower silicon etching rate (<0.6 μm min^{-1}), for example by increasing the amount of DIW used. Since slower silicon etching rates require longer etching time to complete lateral etching, the time of the vertical solution infiltration (5.1 μm min^{-1}) is also set to the same longer time, forming a cone-like tip section of a greater height, which can result in sharper cones. An additional process of cycled thermal oxidation and oxide removal could be used in order to obtain nanotips with curvature radii below 40 nm [16].

Table 1. Sharpening parameters for the tip angles of 38°, 27°, and 11° shown in SEM images of figure 3. (Note: All etching carried out at 40 °C.)

Solution $HF:HNO_3:H_2O$	Silicon etching rate (μm min^{-1})	Etching time (s)	Angle (deg)	Figures
1:50:0	1.1	60	38	3(a)
1:100:0	0.7	85	27	3(b)
1:50:25	0.6	150	11	3(c)

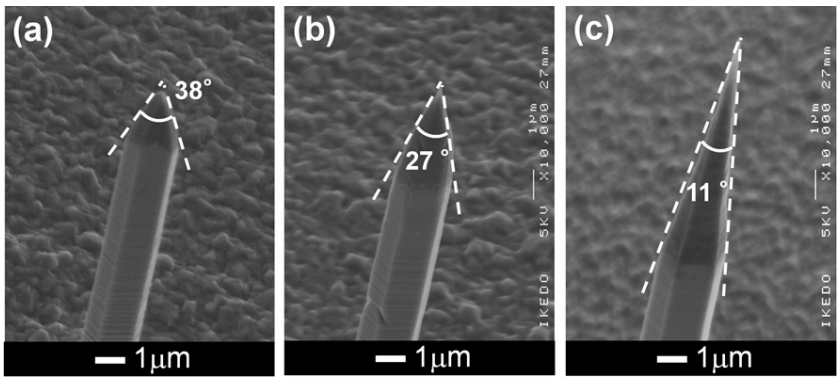

Figure 3. Variation of nanotip angles by altering sharpening parameters. (a) 38° by etching solution of HF:HNO_3:H_2O = 1:50:0 for 60 s, (b) 27° by HF:HNO_3:H_2O ratio of 1:100:0 for 85 s, (c) 11° by HF:HNO_3:H_2O of 1:50:25 for 150 s. All of the sharpening was carried out at 40 °C.

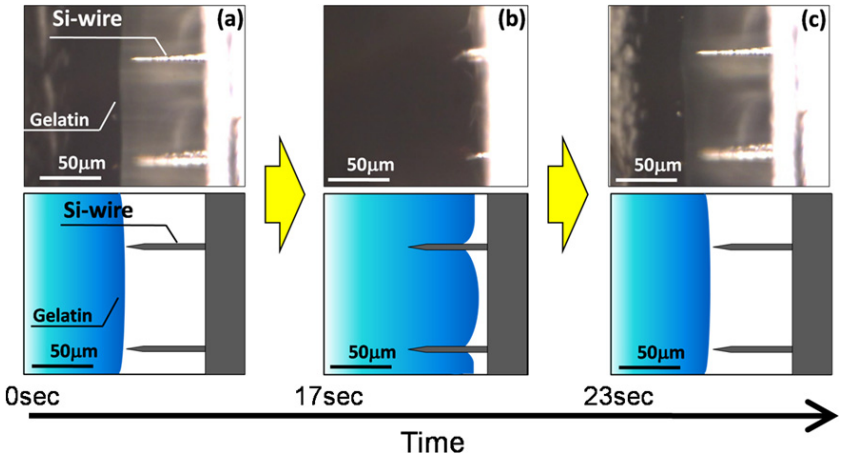

Figure 4. Two nanotip silicon microwires penetrate into a gelatin. (a) Before penetration. (b) During penetration. (c) After extraction from the gelatin. The diameter of the wire scaffold and the tip angle are 2 μm and 11°, respectively, and the overall wire length is 50 μm.

3. Nanotip wire penetration

To confirm the penetration capability and reliability of the resulting arrays into biological tissues, a penetration experiment was demonstrated using a gelatin membrane (6.5 wt% in water) in lieu of neuronal tissue. The hardness of the gelatin was similar to the cardiac muscle of a pig. Figure 4 shows the penetration experiment on two nanotip wires. The wire used consists of a scaffold 2 μm in diameter with an 11° sharpened tip and overall wire length of 50 μm, as shown in figure 3(c). We have demonstrated nanotip wire penetration and extraction without breakage or causing damage to the wires in several continuous tests (more than 10 runs), confirming the penetration capability and reliability of the nanotip wires. We also simulated the pressure distributions of a nanoscale tip wire (100 nm diameter) for a tip reaching a model cell (Poisson's ratio of 0.3, Young's modulus of 5 kPa) [1], by utilizing finite element method analysis (ANSYS). We applied a total force of 1 nN [17] to the model cell through the wire. As we expected, the simulation confirms that the pressure at the cell surface can be increased locally with a nanotip wire, which yields an increased pressure of 3 kPa. This value is about 350 times larger than for a 2 μm diameter tip (cell surface pressure of 0.8 Pa). Based on the results of localized penetration pressure and the predicted advantage of minimal deformation of a biological target (cell/tissue) during penetration [1], the penetrating characteristics of the microwire can be significantly improved by nanotip formation.

4. Conclusion

We have developed a batch process for fabricating nanotip silicon microwire arrays with a high aspect ratio by selective VLS growth of silicon and the subsequent sharpening of the wire tips using chemical etching. The nanoscale sharpening process, based on chemical etching, is repeatable, fast, batch-processable and IC-compatible. In addition, the sharpening process using photoresist spray-coating and plasma etching without additional masking is theoretically a height-independent process. In principle, it could be used for samples with even higher aspect ratios, such as silicon microwires more than 100 μm long, promising simple fabrication of a variety of three-dimensional micro-or nano-devices.

Acknowledgments

The authors gratefully acknowledge K Takei, T Harimoto, A Fujishiro, A Okugawa, Professor A Ishihara and Professor

S Usui for useful discussions, and K Muramoto for his TEM work. This work was supported by the grant for Young Research Projects of the Research Center for Future Technology (Toyohashi University of Technology), a Grant-in-Aid for Scientific Research (S), by the Global COE Program 'Frontiers of Intelligent Sensing' and by the Strategic Research Program for Brain Sciences (SRPBS) from the Ministry of Education, Culture, Sports, Science and Technology of Japan (MEXT).

References

[1] Obataya I, Nakamura C, Han S W, Nakamura N and Miyake J 2005 *Nano Lett.* **5** 27–30
[2] Chen X, Kis A, Zettl A and Bertozzi C R 2007 *Proc. Natl Acad. Sci.* **104** 8218–22
[3] Kouklin N A, Kim W E, Lazareck A D and Xu J M 2005 *Appl. Phys. Lett.* **87** 173901
[4] Freedman J R, Mattia D, Korneva G, Gogotsi Y, Friedman G and Fontecchioa A K 2007 *Appl. Phys. Lett.* **90** 103108
[5] Patolsky F, Timko B P, Yu G, Fang Y, Greytak A B, Zheng G and Lieber C M 2006 *Science* **313** 1100–4
[6] Cohen-Karni T, Timko B P, Weiss L E and Lieber C M 2009 *Proc. Natl Acad. Sci.* **106** 7309–13
[7] Timko B P, Cohen-Karni T, Yu G, Qing Q, Tian B and Lieber C M 2009 *Nano Lett.* **9** 914–8
[8] Hochberg L R, Serruya M D, Friehs G M, Mukand J A, Saleh M, Caplan A H, Branner A, Chen D, Penn R D and Donoghue J P 2006 *Nature* **442** 164–71
[9] Park W I, Zheng G, Jiang X, Tian B and Lieber C M 2008 *Nano Lett.* **8** 3004–9
[10] Hata K, Futaba D N, Mizuno K, Namai T, Yumura M and Iijima S 2004 *Science* **306** 1362–4
[11] Hoffmann S, Utke I, Moser B, Michler J, Christiansen S H, Schmidt V, Senz S, Werner P, Gösele U and Ballif C 2006 *Nano Lett.* **6** 622–5
[12] Wagner R S and Ellis W C 1964 *Appl. Phys. Lett.* **4** 89–90
[13] Kawano T, Kato Y, Futagawa M, Takao H, Sawada K and Ishida M 2002 *Sensors Actuators* A **97** 709–15
[14] Ikedo A, Kawashima T, Kawano T and Ishida M 2009 *Appl. Phys. Lett.* **95** 033502
[15] Schwarts B and Robbins H 1976 *J. Electrochem. Soc.* **123** 1903–9
[16] Marcus R B, Ravi T S, Gmitter T, Chin K, Liu D, Orvis W J, Ciarlo D R, Hunt C E and Trujillo J 1990 *Appl. Phys. Lett.* **56** 236–8
[17] Kojima H, Ishijima A and Yanagida T 1994 *Proc. Natl Acad. Sci.* **91** 12962–6